

## Research highlight

Pooja Puneet, Ramakrishna Podila, Jian He, Apparao M. Rao\*, Austin Howard, Nicholas Cornell and Anvar A. Zakhidov

# Synthesis and superconductivity in spark plasma sintered pristine and graphene-doped $\text{FeSe}_{0.5}\text{Te}_{0.5}$

DOI 10.1515/ntrev-2015-0018

Received March 10, 2015; accepted April 17, 2015; previously published online July 17, 2015

**Abstract:** Here, we present a new ball-milling and spark plasma sintering (SPS)-based technique for the facile synthesis of  $\text{FeSe}_{0.5}\text{Te}_{0.5}$  superconductors without the need for pre-alloying. This method is advantageous since it is quick and flexible for incorporating other dopants such as graphene for vortex pinning. We observed that  $\text{FeSe}_{0.5}\text{Te}_{0.5}$  exhibits a coexistence of ferromagnetic (FM) and superconductivity signature plausibly arising from a FM core-superconducting shell structure. More importantly, the  $H_{c2}$  values observed from resistivity data are higher than 7 T, indicating that SPS process synthesized  $\text{FeSe}_{0.5}\text{Te}_{0.5}$  samples could lead to next-generation superconducting wires and cables.

**Keywords:** graphene; spark plasma sintering; superconductivity.

## 1 Introduction

The discovery of layer structured cuprates, with superconducting transition temperatures ( $T_c$ ) above the liquid-nitrogen temperature, has heralded the search

for high  $T_c$  superconductors which transcend the traditional Bardeen-Cooper-Schrieffer type superconductors. In cuprates, superconductivity evolves from doping of antiferromagnetic Mott insulating phase with excess carriers. Following this discovery, many materials have been found to exhibit superconductivity when their intrinsic long-range magnetic order is suppressed by doping beyond a threshold dopant concentration. In this regard, the recent realization of five different Fe-pnictide superconductors [1–24] in  $\text{LaFeAsO}_{1-x}\text{F}_x$ ,  $\text{BaFe}_2\text{As}_2$ ,  $\text{LiFeAs}$ ,  $\text{Sr}_2\text{PO}_3\text{FePn}$ , and  $\text{FeSe}_x\text{Te}_{1-x}$  systems has reinvigorated the search for new high- $T_c$  non-cuprate materials. While a comprehensive understanding of superconductivity in these systems is still under development, it has been proposed (from an experimental standpoint) that some magnetic fluctuations (e.g. Fe  $3d$  orbital fluctuations across the Fermi energy) may play a similar role as phonons for the formation of Cooper pairs [5]. These unusual electron pairing mechanisms in Fe-based materials, therefore, offer novel insights onto the long-standing fundamental question on the pair mechanism of high- $T_c$  superconductors, cuprates and non-cuprates. Among the five different recently discovered Fe-based superconductors [1–24], FeSe is the only pnictide with a simple crystal structure [1, 3, 6], and is therefore highly suitable for elucidating the fundamental mechanism of superconductivity. Consequently, the crystal structure of FeSe may be easily distorted by external pressure or doping for an increased  $T_c$ . Although many researchers have reported on the influence of doping and external pressure in FeSe materials [6], there are still two major questions that warrant a focused study: (i) from a fundamental perspective, a coherent understanding of the interplay between magnetism and superconductivity still remains to be achieved [1, 3, 6], and (ii) the low critical current density ( $J_c$ ) of FeSe materials is a persisting concern for practical applications [1]. Since  $J_c$  is intimately related to the micro-morphology of grain boundary, it is highly desired to synthesize FeSe materials with controlled grain boundary morphology [1].

**\*Corresponding author: Apparao M. Rao**, Department of Physics and Astronomy, Clemson Nanomaterials Center, Clemson University, Clemson, SC 29634, USA, e-mail: arao@clemson.edu; and Center for Optical Materials Science and Engineering Technologies (COMSET), Clemson, SC 29634, USA

**Pooja Puneet and Jian He:** Department of Physics and Astronomy, Clemson Nanomaterials Center, Clemson University, Clemson, SC 29634, USA

**Ramakrishna Podila:** Department of Physics and Astronomy, Clemson Nanomaterials Center, Clemson University, Clemson, SC 29634, USA; and Center for Optical Materials Science and Engineering Technologies (COMSET), Clemson, SC 29634, USA

**Austin Howard, Nicholas Cornell and Anvar A. Zakhidov:** Nanotech Institute, University of Texas at Dallas, Richardson, TX 75080, USA

In the present work, we address these challenges by employing a novel synthesis technique through ball-milling and subsequent spark plasma sintering (SPS) without any need for pre-alloying. We expect that the SPS method results in lower magnetic impurities and also facilitates the introduction of defects/pinning centers (for example, through the addition of nanomaterials such as graphene). SPS is a high energy, low voltage, pulsed plasma discharge in a low-pressure atmosphere that can generate highly localized Joule heating (up to a few thousand degrees Kelvin) in a few minutes [1, 25, 26]. Here, we employed *in situ* SPS to synthesize the superconducting phase of  $\text{FeSe}_{0.5}\text{Te}_{0.5}$  to simultaneously enhance both the  $T_c$  and  $J_c$ . Moreover, since  $\text{FeSe}_{0.5}\text{Te}_{0.5}$  is a layered material, we included few-layer graphene during the ball-milling and SPS process for creating vortex pinning centers, and exploring the interplay between magnetism and superconductivity. We observed that our samples exhibited a co-existence of ferromagnetic ordering and superconductivity below  $T_c=15$  K. Notably, our magneto-resistance data showed no loss in superconductivity up to 7 T with

a  $<800$  mK shift in  $T_c$ . We explain our results in terms of a self-consistent superconducting shell-magnetic core scheme wherein the shell forms a percolated robust superconducting path.

## 2 Materials and methods

The starting materials for the synthesis of pristine  $\text{FeSe}$  and  $\text{FeSe}_{0.5}\text{Te}_{0.5}$  were as-purchased powders of Fe ( $\sim 100$   $\mu\text{m}$ ,  $>99.9\%$ ), Se ( $\sim 50$   $\mu\text{m}$ ,  $>99.9\%$ ), Te ( $\sim 50$   $\mu\text{m}$ ,  $>99.9\%$ ) from Alfa-Aesar (Ward Hill, MA, USA). These elemental powders were mixed according to the chemical formula to yield  $\text{FeSe}_{0.5}\text{Te}_{0.5}$  in an Ar purged glove box. Subsequently, the powders were ball-milled in a stainless steel container for 15 h under Ar (manufacturer: SPEX sampleprep LLC., Metuchen, NJ, USA) with 1:3 power-to-ball ratio. The ball-milled powders were sintered using the SPS technique at  $700^\circ\text{C}$  for 5 min at a pressure of 50 MPa with ON-OFF ratios of 12:2 and 1:1 (Fuji electronics Co. Ltd., Dr. Sinter, Kanagawa, Japan). Few-layer graphene sheets

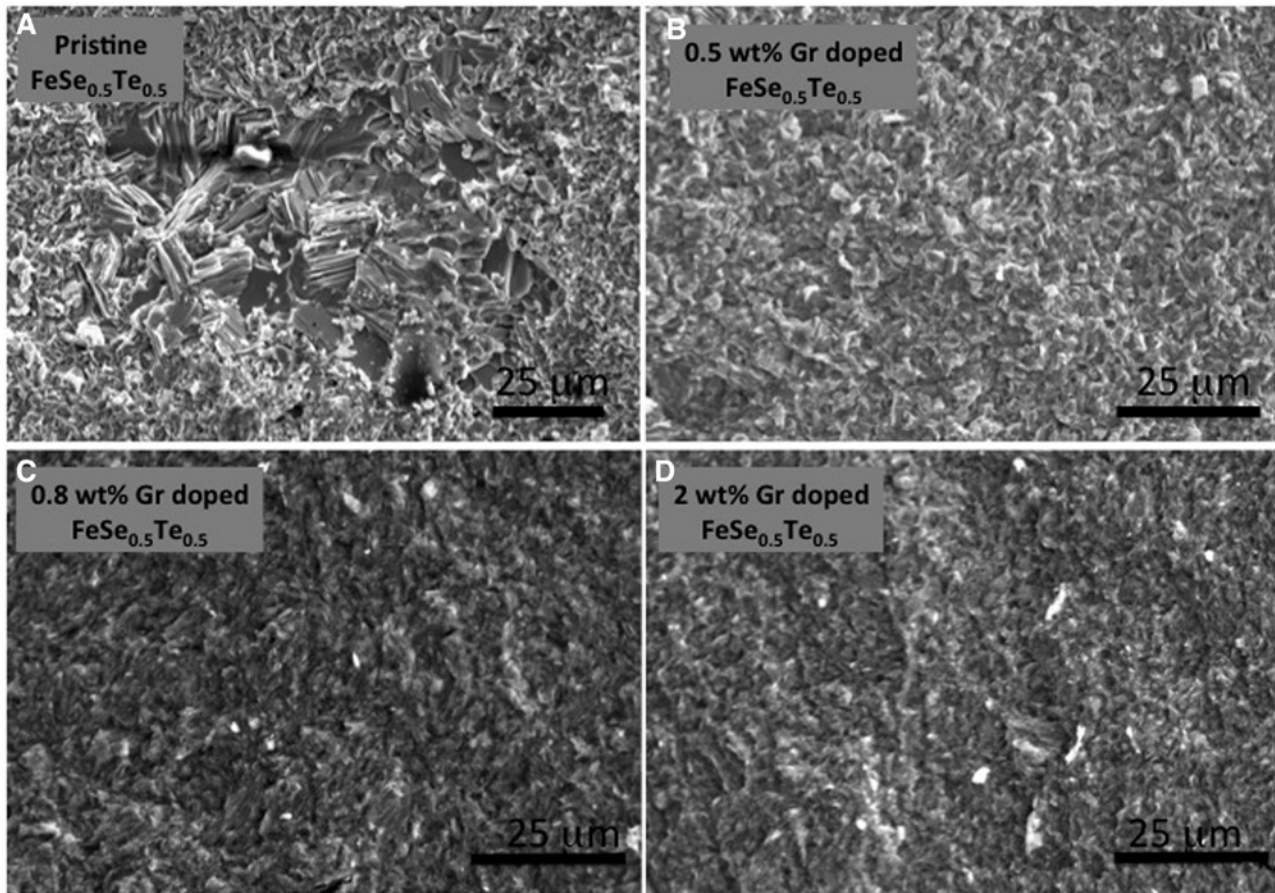


**Figure 1:** Representative scanning electron micrographs for  $\text{FeSe}_{0.5}\text{Te}_{0.5}$  samples with: (A) 0% wt., (B) 0.5% wt., (C) 0.8% wt., and (D) 2% wt. graphene.

were prepared using a chemical exfoliation technique described in Ref. [27].

### 3 Results

As shown in Figure 1, the examination of fractured surface for sintered specimens revealed a poly-crystalline and layered structure for pristine FeSe<sub>0.5</sub>Te<sub>0.5</sub> samples with layers extending to tens of microns. Furthermore, the presence of graphene (0.5–2% wt.) appeared to increase the density (from ~85% to 90% of theoretical density) of sintered samples, indicating a possible lattice distortion. Unlike many previous studies, we used the SPS process to directly synthesize the superconducting phase rather than using it as a mere densification tool. The advantage of this process lies in its high throughput and short timescales (~5–10 min) required for sample preparation without the need for any pre-alloying. The X-ray diffractograms (Supplemental Figure 1) showed that the observed

interplanar distance matches with FeSe<sub>0.5</sub>Te<sub>0.5</sub> in accordance with Vegard's law.

All SPS synthesized samples exhibited a  $T_c$  with a clear signature for ferromagnetism (see Figure 2) both below and above  $T_c$  (~15 K), indicating the co-existence of FM and superconducting domains. The evident drop in resistivity ~15 K (Figure 3) and a simultaneous display of diamagnetic behavior (as shown in Figure 2) confirms the presence of a percolating superconducting path among the FM domains. Interestingly, the magnetic hysteresis did not exhibit much temperature dependence below 15 K. Such an observation may plausibly be attributed to field trapping in FM domains during M-H sweeps above  $T_c$ . The magnetic properties of the FeSe family of compounds are extremely sensitive to the crystal structure, stoichiometry and the presence of excess Fe. For instance, superconductivity in Fe<sub>1.01</sub>Se with  $T_c$  ~8 K is destroyed due to FM ordering introduced by only 0.2 at% increase in Fe, and no superconductivity is observed in Fe<sub>1.03</sub>Se [28]. In this regard, it is possible that any unreacted Fe or formation

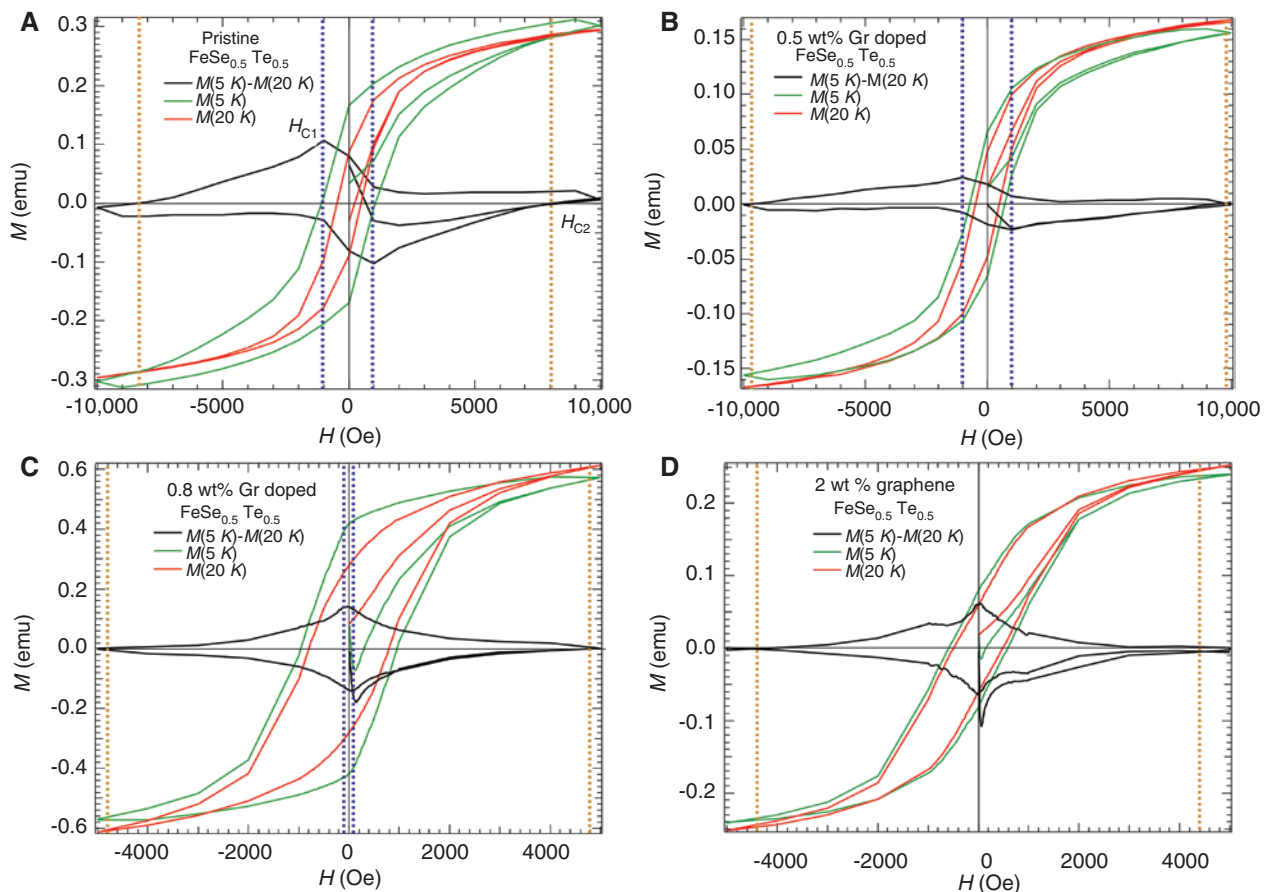


**Figure 2:** Hysteresis loops showing magnetization vs. the applied field for all the FeSe<sub>0.5</sub>Te<sub>0.5</sub> samples with (A) 0% wt., (B) 0.5% wt., (C) 0.8% wt., and (D) 2% wt. graphene. The normalized magnetic moment ( $M_N = M[5\text{ K}] - M[20\text{ K}]$ ) clearly exhibits a shape typical of superconductors showing evident changes at  $H_{c1}$  and  $H_{c2}$  for all samples.

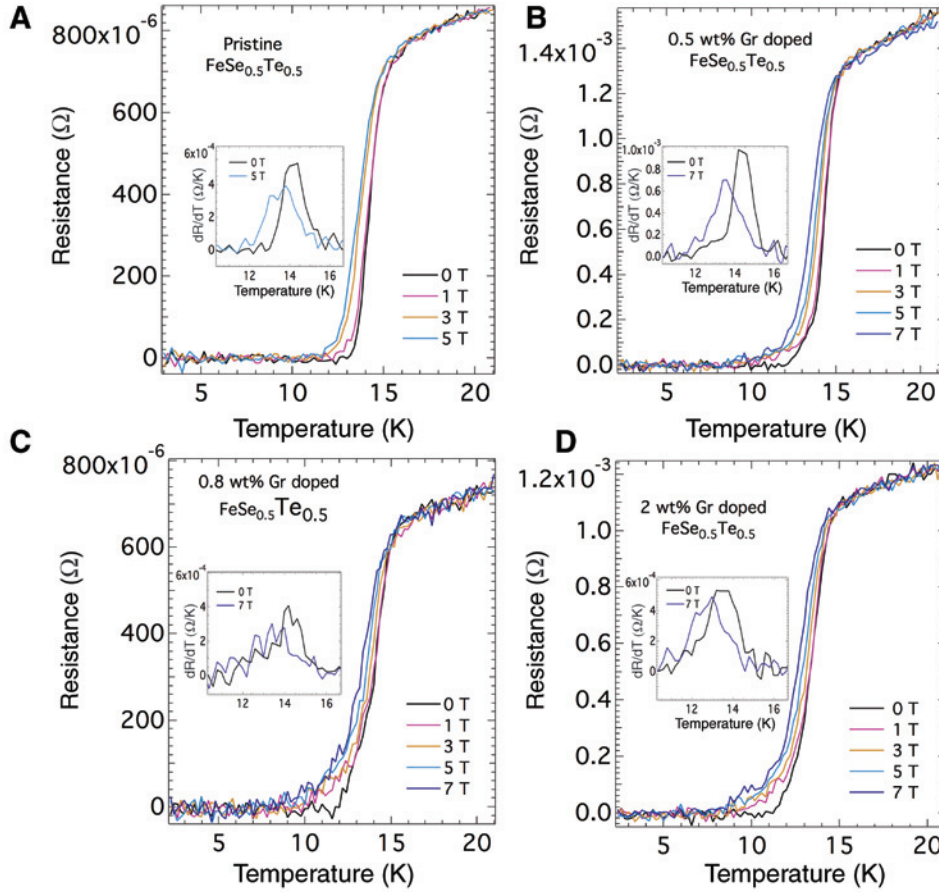


**Figure 3:** Temperature dependent electrical resistivity for all the  $\text{FeSe}_{0.5}\text{Te}_{0.5}$  samples with (A) 0% wt., (B) 0.5% wt., (C) 0.8% wt. and (D) 2% wt. graphene. A transition is observed  $\sim 14.5$  K suggesting that there is a superconducting percolation path in the sample. The insets show the derivative of resistance with respect to temperature and help in clearly identifying  $T_c$ . For all pristine and doped  $\text{FeSe}_{0.5}\text{Te}_{0.5}$  samples, superconductivity (SC) transition was observed up to 7 T suggesting robust superconductivity.

of  $\text{Fe}_{1-y}\text{Se}_y\text{Te}_{0.5}$  phase during the SPS process may contribute to the observed FM signature (Figure 2). Indeed, the nominal composition of our samples lies in the FM ordering and superconductivity overlapping region of the phase diagram of  $\text{Fe}_{1.03}\text{Se}_{0.5}\text{Te}_{0.5}$  described in Ref. [9]. The normalized magnetic moment ( $M_N = M[5\text{ K}] - M[20\text{ K}]$ ) clearly exhibits a shape typical of superconductors showing evident changes at  $H_{c1}$  and  $H_{c2}$  for all samples (Figure 2). While the magnetic data suggests an  $H_{c2}^M$  (i.e.  $H_{c2}$  from magnetic measurements)  $\sim 8\text{--}10$  kOe, the resistivity ( $\rho$ ) data exhibited a clear superconductivity transition  $\sim 14.5$  K in external magnetic fields as high as 7 T (Figure 3). Interestingly,  $H_{c2}^M$  was found to be highest at 0.5% wt. of graphene doping (performed during ball-milling) suggesting that the magnetic vortices can be pinned effectively by graphene at low concentrations  $< 1\%$  wt. (Figure 4). As shown in Figure 3, the superconducting transition persisted even at external fields as high as 7 T in  $\rho(T)$  data suggesting that the  $H_{c2}^R$  [i.e.  $H_{c2}$  from  $\rho(T)$  data measurements] is much higher

than  $H_{c2}^M$ , as observed in other Fe-based superconductive systems. Such an observation may plausibly be attributed to the presence of magnetic domains that result in a pseudo  $H_{c2}$  value in M-H measurements shown in Figure 2. As shown in the insets of Figure 3A–D, we determined  $T_c$  values by identifying the peak position of  $d\rho(T)/dT$ . We observed that graphene dopants increased  $T_c$  of  $\text{FeSe}_{0.5}\text{Te}_{0.5}$  samples at low concentrations ( $< 1\%$  wt.) by 200 mK (Figure 4). The net shift in  $T_c$  ( $\Delta T_c = T_c[0\text{ T}] - T_c[7\text{ T}]$ ) upon the application of external field was found to be within 400–800 mK suggesting a robust superconducting percolated transport path in our samples.

The pulsed direct current (DC) method of energizing in the SPS method activates particulate surfaces by removing either impurities or oxidation layers through electric discharges between neighboring particulates in addition to Joule heating at the grain boundaries. In the SPS process, the applied DC pulses are square/rectangular waveforms with different ON-OFF durations. The ON

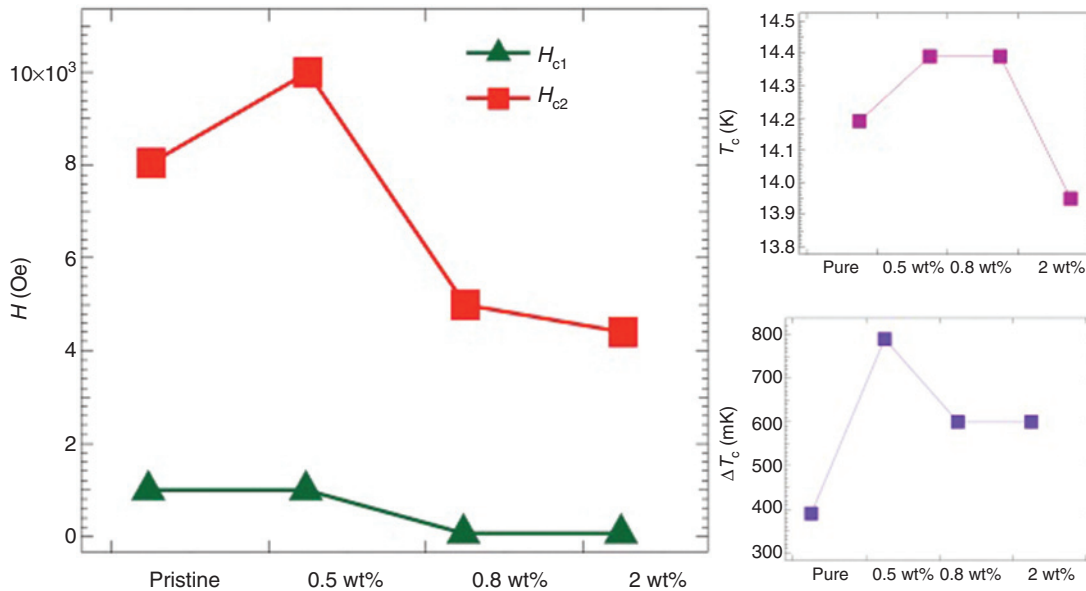


**Figure 4:** The effect of graphene doping on critical fields  $H_{c1}$  and  $H_{c2}$  (obtained from magnetism measurements) and  $T_c$  obtained from the plots shown in Figures 2 and 3.

time activates the particulates while the OFF time allows relaxation of the sintered material during the sintering process. Hence, the ON-OFF time ratio of x:y suggests that there are x ON current pulses with y OFF pulses used during the sintering process. The time duration of each ON or OFF pulse is 2.7 ms (for further details, see SPS standard Procedure, Dr. Sinter SPS, Service Manual No. 16). It is well-known that a change in SPS ON-OFF conditions can significantly influence material properties such as electrical resistivity, mechanical robustness and thermopower. In this regard, to study the effect of SPS pulse conditions, we prepared FeSe<sub>0.5</sub>Te<sub>0.5</sub> samples at 12:2 and 1:1 ON-OFF ratios. Interestingly, we did not observe any differences in the magnetic and electrical transport between these samples, suggesting that the superconductivity in our samples is robust.

Juxtaposing the data from magnetic, transport and SPS ON-OFF ratios, we propose a superconducting shell-FM core structure (see Figure 5) with a percolated conductive path among the superconducting shells. Since Fe is more conducting than Se and Te, it is expected that the DC passes mainly through Fe powders. As shown in Figure 5, such a condition results in the formation of a FeSe<sub>0.5</sub>Te<sub>0.5</sub> shell with some unreacted or partly reacted Fe, Se, and Te forming a FM core. While the cores exhibit traditional FM ordering above  $T_c$ , any trapped field can result in a remnant magnetization below  $T_c$  despite the shielding of FM cores by superconducting shells. In the case of low graphene dopant concentrations, graphene is possibly present at

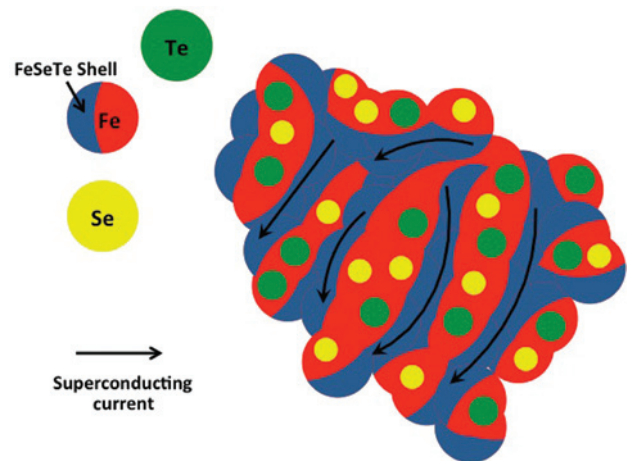


**Figure 5:** A schematic of the FeSe<sub>0.5</sub>Te<sub>0.5</sub> sample formed through ball-milling and spark plasma sintering (SPS).

the interfaces between the FM core and superconducting shells acting as a pinning center that prevents the vortices from spreading into the superconducting path.

## 4 Conclusion

In summary, we present a new ball-milling and SPS-based technique for the facile synthesis of FeSe<sub>0.5</sub>Te<sub>0.5</sub> samples without any pre-alloying. We observed that FeSe<sub>0.5</sub>Te<sub>0.5</sub>

exhibits a coexistence of FM ordering and superconductivity signature plausibly arising from a FM core-superconductivity shell structure. We doped the samples with graphene during the synthesis process for vortex pinning. We found that graphene could be doped up to 2% wt. using ball-milling and the SPS method, but did not show any significant effects on the  $T_c$ . Interestingly, 0.5% wt. of graphene resulted in a slight increase (~400 mK) in  $T_c$  while doping above 0.5% wt. deteriorated the superconductive properties. For all the doping ratios, we observed that the superconducting transition in electrical transport measurements is robust up to 7 T.

**Acknowledgments:** AMR and AZ are thankful to the Air Force Office of Scientific Research (AFOSR) grant on superconductivity. AMR, JH, and RP thank Clemson University TIGER grant for supporting this work.

## References

- [1] Ahn JH, Oh S. Effect of hot-consolidation method on the superconducting properties of B- and C-doped FeSe<sub>0.5</sub>Te<sub>0.5</sub>. *Curr. Appl. Phys.* 2013, 13, 1096–1100.
- [2] Bao W, Qiu Y, Huang Q, Green MA, Zajdel P, Fitzsimmons MR, Zhernenkov M, Chang S, Fang MH, Qian B, Vohstedt EK, Yang JH, Pham HM, Spinu L, Mao ZQ. Tunable ( $\delta$  pi,  $\delta$  pi)-type antiferromagnetic order in alpha-Fe(Te,Se) superconductors. *Phys. Rev. Lett.* 2009, 102, 247001.
- [3] Bellingeri E, Buzio R, Gerbi A, Marre D, Congiu S, Cimberle MR, Tropeano M, Siri AS, Palenzona A, Ferdeghini C. High quality epitaxial FeSe<sub>0.5</sub>Te<sub>0.5</sub> thin films grown on SrTiO<sub>3</sub> substrates by pulsed laser deposition. *Supercond. Sci. Technol.* 2009, 22, 105007.
- [4] Chen GF, Li Z, Wu D, Li G, Hu WZ, Dong J, Zheng P, Luo JL, Wang NL. Superconductivity at 41 K and its competition with spin-density-wave instability in layered CeO(1-x)F(x)FeAs. *Phys. Rev. Lett.* 2008, 100, 247002.
- [5] Chubukov AV, Efremov DV, Eremin I. Magnetism, superconductivity, and pairing symmetry in iron-based superconductors. *Phys. Rev. B.* 2008, 78, 134512.
- [6] Hsu FC, Luo JY, Yeh KW, Chen TK, Huang TW, Wu PM, Lee YC, Huang YL, Chu YY, Yan DC, Wu MK. Superconductivity in the PbO-type structure alpha-FeSe. *Proc. Natl. Acad. Sci. USA* 2008, 105, 14262–14264.
- [7] Jaroszynski J, Hunte F, Balicas L, Jo YJ, Raicevic I, Gurevich A, Larbalestier DC, Balakirev FF, Fang L, Cheng P, Jia Y, Wen HH. Upper critical fields and thermally-activated transport of NdFeAsO<sub>0.7</sub>F<sub>0.3</sub> single crystal. *Phys. Rev. B.* 2008, 78, 174523.
- [8] Kamihara Y, Watanabe T, Hirano M, Hosono H. Iron-based layered superconductor LaO<sub>1-x</sub>F<sub>x</sub>FeAs (x=0.05-0.12) with T<sub>c</sub>=26 K. *J. Am. Chem. Soc.* 2008, 130, 3296–3297.
- [9] Khasanov R, Bendele M, Amato A, Babkevich P, Boothroyd AT, Cervellino A, Conder K, Gvasaliya SN, Keller H, Klauss HH, Luetkens H, Pomjakushin V, Pomjakushina E, Roessli B. Coexistence of incommensurate magnetism and superconductivity in Fe(1+y)SexTe(1-x). *Phys. Rev. B.* 2009, 80, 140511.
- [10] Li SL, de la Cruz C, Huang Q, Chen Y, Lynn JW, Hu JP, Huang YL, Hsu FC, Yeh KW, Wu MK, Dai PC. First-order magnetic and structural phase transitions in Fe<sub>1+y</sub>SexTe<sub>1-x</sub>. *Phys. Rev. B.* 2009, 79, 54503.
- [11] Lv B, Gooch M, Lorenz B, Chen F, Guloy AM, Chu CW. The superconductor KxSr<sub>1-x</sub>Fe(2)As(2): normal state and superconducting properties. *New J. Phys.* 2009, 11, 2501.
- [12] Martinelli A, Ferretti M, Manfrinetti P, Palenzona A, Tropeano M, Cimberle MR, Ferdeghini C, Valle R, Bernini C, Putti M, Siri AS. Synthesis, crystal structure, microstructure, transport and magnetic properties of SmFeAsO and SmFeAs(O(0.93)F(0.07)). *Supercond. Sci. Technol.* 2008, 21, 95017.
- [13] Matusiak M, Plackowski T, Bukowski Z, Zhigadlo ND, Karpinski J. Evidence of spin-density-wave order in RFeAsO<sub>1-x</sub>F<sub>x</sub> from measurements of thermoelectric power. *Phys. Rev. B.* 2009, 79, 212502.
- [14] Mazin II, Singh DJ, Johannes MD, Du MH. Unconventional superconductivity with a sign reversal in the order parameter of LaFeAsO(1-x)F(x). *Phys. Rev. Lett.* 2008, 101, 57003.
- [15] Mishra V, Boyd G, Graser S, Maier T, Hirschfeld PJ, Scalapino DJ. Lifting of nodes by disorder in extended-s-state superconductors: Application to ferropnictides. *Phys. Rev. B.* 2009, 79, 94512.
- [16] Mizuguchi Y, Tomioka F, Tsuda S, Yamaguchi T, Takano Y. Superconductivity at 27 K in tetragonal FeSe under high pressure. *Appl. Phys. Lett.* 2008, 93, 152505.
- [17] Pallecchi I, Fanciulli C, Tropeano M, Palenzona A, Ferretti M, Malagoli A, Martinelli A, Sheikin I, Putti M, Ferdeghini C. Upper critical field and fluctuation conductivity in the critical regime of doped SmFeAsO. *Phys. Rev. B.* 2009, 79, 104515.
- [18] Pallecchi I, Lamura G, Tropeano M, Putti M, Viennois R, Gianini E, Van der Marel D. Seebeck effect in Fe<sub>1+x</sub>Te<sub>1-y</sub>Se<sub>y</sub> single crystals. *Phys. Rev. B.* 2009, 80, 214511.
- [19] Pinsard-Gaudart L, Berardan D, Bobroff J, Dragoë N. Large Seebeck coefficients in iron-oxypnictides: a new route towards n-type thermoelectric materials. *Phys. Status Solidi RRL.* 2008, 2, 185–187.
- [20] Ren ZA, Yang J, Lu W, Yi W, Shen XL, Li ZC, Che GC, Dong XL, Sun LL, Zhou F, Zhao ZX. Superconductivity in the iron-based F-doped layered quaternary compound NdO(1-x)F(x)FeAs. *Europhys. Lett.* 2008, 82, 57002.
- [21] Sanna S, De Renzi R, Lamura G, Ferdeghini C, Palenzona A, Putti M, Tropeano M, Shiroka T. Magnetic-superconducting phase boundary of SmFeAsO<sub>1-x</sub>F<sub>x</sub> studied via muon spin rotation: Unified behavior in a pnictide family. *Phys. Rev. B.* 2009, 80, 052503.
- [22] Singh DJ, Du MH. Density functional study of LaFeAsO(1-x)F(x): a low carrier density superconductor near itinerant magnetism. *Phys. Rev. Lett.* 2008;100, 237003.
- [23] Takahashi H, Igawa K, Arii K, Kamihara Y, Hirano M, Hosono H. Superconductivity at 43 K in an iron-based layered compound LaO<sub>1-x</sub>F<sub>x</sub>FeAs. *Nature* 2008, 453, 376–378.
- [24] Wen HH, Mu G, Fang L, Yang H, Zhu XY. Superconductivity at 25 K in hole-doped (La(1-x)Sr<sub>4</sub>(x))OFeAs. *Europhys. Lett.* 2008, 82, 17009.
- [25] Puneet P, Podila R, Zhu S, Skove MJ, Tritt TM, He J, Rao AM. Enhancement of thermoelectric performance of ball-milled

bismuth due to spark-plasma-sintering-induced interface modifications. *Adv. Mater.* 2013, 25, 1033–1037.

- [26] Puneet P, Podila R, Karakaya M, Zhu S, He J, Tritt TM, Dresselhaus MS, Rao AM. Preferential scattering by interfacial charged defects for enhanced thermoelectric performance in few-layered n-type  $\text{Bi}_2\text{Te}_3$ . *Sci. Rep.* 2013, 3, 3212.
- [27] Podila R, Vedantam P, Ke PC, Brown JM, Rao AM. Evidence for charge-transfer-induced conformational changes in carbon nanostructure–protein corona. *J. Phys. Chem. C* 2012, 116, 22098–22103.
- [28] McQueen TM, Huang Q, Ksenofontov V, Felser C, Xu Q, Zandbergen H, Hor YS, Allred J, Williams AJ, Qu D, Checkelsky J, Ong NP, Cava RJ. Extreme sensitivity of superconductivity to stoichiometry in  $\text{Fe}_{1+\delta}\text{Se}$ . *Phys. Rev. B* 2009, 79, 014522.

---

**Supplemental Material:** The online version of this article (DOI: 10.1515/ntrev-2015-0018) offers supplementary material, available to authorized users.